CLINICAL AND VACCINE IMMUNOLOGY, May 2008, p. 783–793 Vol. 15, No. 5
1556-6811/08/$08.00+0 doi:10.1128/CVI.00480-07

Live *Mycobacterium avium* subsp. *paratuberculosis* and a Killed-Bacterium Vaccine Induce Distinct Subcutaneous Granulomas, with Unique Cellular and Cytokine Profiles[▽]

Liying Lei,[1,2] Brandon L. Plattner,[2] and Jesse M. Hostetter[1,2]*

Immunobiology Graduate Program[1] and Department of Veterinary Pathology, College of Veterinary Medicine, Iowa State University, Ames, Iowa[2]

Received 7 December 2007/Returned for modification 2 January 2008/Accepted 5 March 2008

Type II (lepromatous) granulomas are characterized by a lack of organization, with large numbers of macrophages heavily burdened with bacilli and disorganized lymphocyte infiltrations. Type II granulomas are a characteristic feature of the enteric lesions that develop during clinical *Mycobacterium avium* subsp. *paratuberculosis* infection in the bovine. Considering the poor organization and function of these granulomas, it is our hypothesis that dendritic cell (DC) function within the granuloma is impaired during initial infection. In order to test our hypothesis, we used a subcutaneous *M. avium* subsp. *paratuberculosis* infection model to examine early DC function within *M. avium* subsp. *paratuberculosis*-induced granulomas. In this model, we first characterized the morphology, cellular composition, and cytokine profiles of subcutaneous granulomas that develop 7 days after subcutaneous inoculation with either vaccine or live *M. avium* subsp. *paratuberculosis*. Second, we isolated CD11c$^+$ cells from within granulomas and measured their maturation status and ability to induce T-cell responses. Our results demonstrate that *M. avium* subsp. *paratuberculosis* or vaccine administration resulted in the formation of distinct granulomas with unique cellular and cytokine profiles. These distinct profiles corresponded to significant differences in the phenotypes and functional responses of DCs from within the granulomas. Specifically, the DCs from the *M. avium* subsp. *paratuberculosis*-induced granulomas had lower levels of expression of costimulatory and chemokine receptors, suggesting limited maturation. This DC phenotype was associated with weaker induction of T-cell proliferation. Taken together, these findings suggest that *M. avium* subsp. *paratuberculosis* infection in vivo influences DC function, which may shape the developing granuloma and initial local protection.

Granulomatous inflammation is the defining lesion of mycobacterial infections (45). The organization and the cellular constituents of the developing granulomas vary with the type of mycobacterial pathogen and the status of the host immune response (1, 12). Broadly, granulomatous lesions can be categorized within two polar forms, both of which include infiltrations of macrophages and lymphocytes. Type I (tuberculoid) granulomas are organized nodular lesions with epithelioid and multinucleated giant cells in the lesion center surrounded by a rim of fibrous connective tissue. Aggregates of lymphocytes are often present around granuloma vasculature and along the granuloma periphery. The core of the type I granuloma may be necrotic, with mineralization. The pathogen burden of the type I granuloma is often low. The type II (lepromatous) granuloma is characterized by a lack of organization, with very large numbers of macrophages heavily burdened with bacilli intermixed with disorganized lymphocyte infiltrations. Overall, there is significant variation in granuloma morphology, with many granulomas having morphology intermediate between types I and II. The morphology of granulomas is important because type I granulomas can be associated with control of pathogen replication, while type II granulomas are associated with extensive pathogen proliferation and disease progression (12, 22). It is now known that granuloma morphology is influenced by the balance between Th1 and Th2 responses and that cytokines associated with Th1 responses drive type I granuloma development (40, 50).

The recruitment of progressive waves of immune cells to an infection site is driven by a complex array of cytokines and chemokines produced by multiple cell types, including macrophages and dendritic cells (DC). Tumor necrosis factor alpha (TNF-α) is an extensively studied cytokine in granuloma formation and appears to be a critical cytokine in the maintenance of granuloma structure (3, 15, 26, 43). Macrophages and DC are important sources of TNF-α (46, 49). TNF-α acts as a positive feedback signal for infected DC and macrophages to secrete more TNF-α, as well as chemokines, including CCL2 and CXCL10, and cytokines, including interleukin-1 (IL-1) and IL-18. These proinflammatory mediators drive the recruitment of CD4$^+$ T cells, CD8$^+$ T cells, monocytes, neutrophils, and natural killer (NK) cells (2). Recruited immune cells further elicit cytokines and chemokines that amplify the cascade of cell infiltration to the infection site and drive granuloma formation (14, 52). Thus, TNF-α coordinates the cascade of cellular infiltrates and inflammatory mediators in the developing granuloma. Interestingly, the regulation of this cascade requires a proinflammatory cytokine, gamma interferon (IFN-γ), for negative feedback. Mice with disrupted IFN-γ gene expression were unable to regulate this response and developed disseminated tuberculosis with marked tissue damage from excessive

* Corresponding author. Mailing address: 2720 Veterinary Medicine, Department of Veterinary Pathology, College of Veterinary Medicine, Iowa State University, Ames, IA 50011-1250. Phone: (515) 294-3282. Fax: (515) 294-5423. E-mail: jesseh@iastate.edu.

▽ Published ahead of print on 12 March 2008.

granuloma formation (8). In addition, tuberculosis reactivation has been a complication of anti-TNF therapy (infliximab and adalimumab) in patients with rheumatoid arthritis, Crohn's disease, and psoriasis (11, 18, 26, 39). Taken together, these observations confirm the essential role of TNF-α in maintaining granuloma function during *Mycobacterium tuberculosis* infection.

It has recently been reported that DC are present in granulomatous lesions (6, 19, 51). Foamy cells within lung granulomas of mice infected with *M. tuberculosis* expressed the characteristic DC markers CD205, major histocompatibility complex class II (MHC-II), CD11c, and CD40 at high levels (35). In a rat model, DC accumulated along the periphery of the *Mycobacterium bovis* BCG-induced pulmonary granulomas, where they expressed high levels of MHC-II, CD80, and CD86 and had potent capacity to induce purified protein derivative (PPD)-specific T-lymphocyte proliferation (51). It has recently been reported that collections of antigen-presenting cells are within close proximity to proliferating lymphocytes in pulmonary granulomas of tuberculosis patients. The results of the study suggested that the interaction of antigen-presenting cells, including DC, with local lymphoid cells is a local regulator of granuloma function (49). Taken together, the results of these studies suggest that DC play a role in the formation and organization of granulomas.

Type II granulomas are a characteristic feature of the enteric lesions that develop during clinical *Mycobacterium avium* subsp. *paratuberculosis* infection in the bovine. In the natural infection, these granulomas can expand throughout the intestinal wall, with eventual loss of mucosal function, and yield very high intracellular bacterial loads. Considering the poor organization and function of these granulomas, it is our hypothesis that DC function is impaired early during *M. avium* subsp. *paratuberculosis*-induced granuloma development. In order to test our hypothesis, we used a subcutaneous *M. avium* subsp. *paratuberculosis* infection model developed by Simutis et al., with modifications (47). This model is beneficial because it was designed for measurement of the early stages of granuloma development after infection with *M. avium* subsp. *paratuberculosis*, including antigen-presenting-cell function at the initial infection site. Using this model, it is possible to induce differential granulomas, with the *M. avium* subsp. *paratuberculosis* vaccine (Mycopar) inducing an organized type I granuloma and live *M. avium* subsp. *paratuberculosis* a granuloma with type II features by 30 days postinoculation (24, 47). In this study, we first characterized the morphology, cellular composition, and cytokine profiles of subcutaneous granulomas that developed 7 days after exposure to vaccine or live *M. avium* subsp. *paratuberculosis*. Second, we isolated $CD11c^+$ cells from within granulomas and measured their maturation status and ability to induce T-cell responses. Our results demonstrate that live *M. avium* subsp. *paratuberculosis* cells induce the formation of a disorganized granulomatous lesion at subcutaneous inoculation sites early after infection. The *M. avium* subsp. *paratuberculosis* granulomas have cellular composition and cytokine profiles that are distinct from those of the vaccine granulomas. We also provide evidence that there is limited maturation and function of DC within the *M. avium* subsp. *paratuberculosis* granulomas. This suggests that DC may play a role in the pathogenesis of *M. avium* subsp. *paratuberculosis* infection by having a limited ability to contribute to the early protective response at the infection site.

MATERIALS AND METHODS

Animals. Four- to 6-week-old Holstein calves were used in the following experiments and were housed in isolation in the Iowa State University College of Veterinary Medicine biosafety level II animal care facility during the study. A total of six animals were used for this project, and three at a time for handling purposes. These animals were maintained free of infection other than the inoculum given in the study. All live-animal-related protocols were approved by the Committee on Animal Care and Use at Iowa State University.

Bacterial inoculum and infection. The *M. avium* subsp. *paratuberculosis* 19698 strain was obtained from the American Type Culture Collection (Manassas, VA) and maintained in Middlebrook 7H9 broth supplemented with mycobactin J. Log-phase-growing live *M. avium* subsp. *paratuberculosis* cells were washed and resuspended in sterile saline for use in in vivo infection. The concentration of bacteria was determined by measuring absorbance at 540 nm and comparing the absorbance optical density value against the standard curve as described previously (5). The *M. avium* subsp. *paratuberculosis* inoculum used in these studies was shown to be above 90% viable as checked via fluorescein diacetate staining and flow cytometry analysis (20, 48). Two animals were given an injection of 5×10^8 CFU live *M. avium* subsp. *paratuberculosis* cells subcutaneously on the neck at day 0.

Vaccine. *M. avium* subsp. *paratuberculosis* vaccine (Mycopar) from Fort Dodge Animal Health was used. Mycopar is a whole-cell bacterin containing inactivated *M. avium* subsp. *paratuberculosis* bacteria. Mycopar generates a granuloma in vivo, and such a result was used as an example of a tuberculoid-type granuloma. Four animals were injected with 0.25 ml of the *M. avium* subsp. *paratuberculosis* vaccine subcutaneously on the neck on day 0.

Granuloma cell isolation. Palpable lesions were present at both live-*M. avium* subsp. *paratuberculosis*-cell and vaccine injection sites at 7 days postinoculation and were removed surgically for analysis. Lesions were fixed in liquid nitrogen or formalin or transported fresh in cold RPMI 1640 medium for cell isolation.

Granuloma cells were isolated by mincing granulomatous tissue and digesting it with 0.25% type IV-S collagenase (from *Clostridium histolyticum*; Sigma) in complete medium for 30 min at 37°C on a shaker. Complete medium is prepared by adding 10% fetal bovine serum, 0.5 mM 2-mercaptoethanol, penicillin G (100 U/ml), streptomycin (100 μg/ml), amphotericin B (250 ng/ml), 2 mM L-glutamine to RPMI 1640 medium. Collagenase treatment was followed by gentle homogenization to completely release cells from granuloma. Granuloma single-cell suspension was washed and counted. An amount of 10^6 to 10^8 cells with more than 90% cell viability was the typical yield from a single granuloma. Total granuloma cells were then divided into groups for cell composition analysis and for $CD11c^+$-cell separation.

PBMC lymphocyte isolation. Peripheral blood mononuclear cells (PBMC) were isolated by density gradient centrifugation on Histopaque (1.083 g/ml; Sigma) and were collected from the interphase. In order to isolate lymphocytes to be used in the proliferation assays, total PBMC were plated overnight in tissue culture flasks in complete medium to allow plastic adherence of monocytes. Nonadherent lymphocytes were washed off of the flasks and collected on the second day.

Antibodies, reagents, and flow cytometry. Granuloma cells were incubated with the relevant monoclonal antibody (MAb), anti-bovine CD11c (BAQ153A; VMRD), CD205 (CC98; Serotec), CD14 (M-M8; VMRD), B cell (B-B4, BAQ155A; VMRD), CD4 (CACT138A; VMRD), CD8-β (BAT82A; VMRD), MHC-I (H58A; VMRD), MHC-II (TH81A5; VMRD), and anti-human CD68 (EBM11; Dako), which had been diluted in fluorescein-activated cell sorter buffer (phosphate-buffered saline containing 1% bovine serum albumin and 0.05% sodium azide). Proper isotype controls were used at the same concentration as the antibody of interest in the study, including MOPC-31C (immunoglobulin G1 [IgG1]), MPC-11 (IgG2b), G155-178 (IgG2a), and G155-228 (IgM) (BD Pharmingen). Cells were then labeled with fluorescein isothiocyanate-conjugated anti-IgG (Invitrogen), phycoerythrin (PE)-conjugated anti-IgG (Invitrogen), or PE-conjugated anti-IgM secondary antibodies (BD Pharmingen). Labeled cells were fixed in 2% paraformaldehyde and analyzed via flow cytometry. Gates were set based on the forward- and side-scatter profiles. The data were collected and analyzed using CellQuest (BD Bioscience) and FlowJo software (Tree Star, Inc.).

Histology, immunohistochemistry, and lesion scoring. Granulomatous-lesion sections were stained with hematoxylin and eosin (H&E) or reserved for immunohistochemistry staining for CD4, CD68, and CD11c. Cryosections were fixed in either cold acetone (CD11c) or cold ethanol (CD4). Formalin-fixed granuloma

TABLE 1. Primer sequences for qRT-PCR

Gene product	Primer		GenBank accession no.
	Sense	Antisense	
CCR7	ATTTGCTTCGTGGGCCTTCT	CATGGTCTTGAGCCTCTTGAAA	AY834253
CD40	GGGCTTTTGGATACCGTCTGT	AGCAGATGACACGTTGGAGAAG	U57745
CD80	CCATCCTGCCTGGAAAAGTG	GGTTATCGTTCATGTCAGTGATGGT	Y099950
CD86	TGTGTGCAGGCCTTCAACA	CGGCCTTAAGTCCATTTGGTT	AJ291475
IL-10	GCCTTGTCGGAAATGATCCA	ATGTCAGGCCCGTGGTTCT	NM174088
IFN-γ	CAGAAAGCGGAAGAGAAGTCAGA	GCAGGAGGACCATTACGTTGA	M29867
TNF-α	GCTGGTTGTCTTCCAGCTTCA	CGGTGGTGGGACTCGTATG	NM173966
TGF-β	CATCTGGAGCCTGGATACACAGT	GAAGCGCCCGGGTTGT	M36271
IL-4	GGAGCCACACGTGCTTGAA	TGCTTGCCAAGCTGTTGAGA	NM173921
IL-12p40	CAACGTCCGCGTGCAA	GCAGGACACAGATGCCCATT	U11815
IL-18	TCCGGACTGGCAGACAGTTC	CCCTTCAGCAGCAGAAGCA	BC102879
IL-12p35	GGAAGGAGCTGCCTCGACTA	TGGCCTTCTGTAGCGTGTTG	U14416
β-Actin	CGCCATGGATGATGATATTGC	AAGCCGGCCTTGCACAT	AF191490

lesions were used for the CD68 stain. Mouse anti-bovine CD4 (IL-A11; VMRD), mouse anti-bovine CD11c (BAQ153A; VMRD), and mouse anti-human CD68 (EBM11; Dako), respectively, were used as primary antibodies. The secondary antibodies included biotinylated goat anti-mouse IgG and anti-mouse IgM MAbs. This incubation was followed by treatment with streptavidin-horseradish peroxidase (Zymed) and substrate 3,3′-diaminobenzidine and color development.

H&E-stained granulomatous lesions were individually scored using a scoring system adapted from previous publications (17, 21, 55). Briefly, scores of 0 to 3 were assigned for individual parameters to reflect the degree and organization of that particular parameter within the lesion. A score of 0 indicates that the parameter was absent from the lesion, while a score of 3 indicates a high degree of organization of the parameter in any given lesion. The following parameters were included: mature fibrous connective tissue, macrophages, lymphocytes, multinucleated giant cells, necrosis, and mineralization. Individual parameters were summated, and a single collective score was assigned for each lesion which reflected the histological organization or stage of development of the individual lesion. A saline control site was included as a negative control and was devoid of significant inflammation.

CD11c$^+$-cell isolation. Total granuloma cells were labeled with anti-bovine CD11c MAb (IgM), followed by anti-IgM magnetic beads. CD11c$^+$ cells were positively selected by using an automagnetic cell-sorting (AutoMACS) separation column (Miltenyi Biotec). The purity of CD11c$^+$ cells isolated by this method was above 90% as confirmed by flow cytometry.

LCM of immunofluorescence-stained frozen tissue. A frozen granulomatous lesion was cut at 6 μm and immunofluorescence labeled for CD11c. Alexa Fluor 488 anti-mouse IgM (A21042; Invitrogen) was used as the secondary antibody for this purpose. Green-fluorescence-positive CD11c cells were captured via laser capture microdissection (LCM) and used for RNA isolation. For the isolation of total granuloma cells, all of the immune cells inside granuloma cryosections were captured using LCM. Total RNA from either CD11c$^+$ cells or total granuloma cells was extracted by using a PicoPure RNA isolation kit (Molecular Devices). The quantity and quality of the RNA were determined by using NanoDrop ND-1000.

Quantitative real-time reverse transcriptase PCR (qRT-PCR). Possible genomic DNA contamination in the RNA samples was eliminated by using Turbo DNA-free (Ambion). A SuperScript III first-strand synthesis system for RT-PCR (Invitrogen) was used for cDNA synthesis. A Sybr green PCR system (Applied Biosystems) was used in the two-step real-time PCR, and the signal was detected by using a GeneAmp 5700 sequence detection system. Dissociation curve analysis was conducted as an appropriate control for each target gene. The primer sequences, designed by using Primer Express Software (Applied Biosystems), and GenBank accession numbers are listed in Table 1.

The relative quantification of target gene mRNA was analyzed using the following equation, modified based on the Pfaffl method (30, 38). β-Actin was used as the internal control reference gene. N_0 represents the original copy number. C_T is the threshold cycle. $N_{0\ \text{target}}/N_{0\ \text{reference}} = (1 + \text{Efficiency}_{\text{reference}})^{CT\ \text{reference}}/(1 + \text{Efficiency}_{\text{target}})^{CT\ \text{target}}$.

PPD antigen-specific CD4$^+$ T-lymphocyte proliferation induced by granuloma CD11c$^+$ cells. Isolated CD11c$^+$ cells from either vaccine- or *M. avium* subsp. *paratuberculosis*-induced granulomas were incubated overnight in medium containing 10 μg/ml PPD. PPD-pulsed granuloma CD11c$^+$ cells were then added to a 96-well round-bottomed plate. Lymphocytes were separated from PBMC and were labeled with PKH67 green-fluorescent-cell linker (PKH67; Sigma). Amounts of 2×10^5 lymphocytes were added to plates with 2×10^4 CD11c$^+$ cells for a final lymphocyte/DC ratio of 10:1. CD11c$^+$ cells and lymphocytes from the same animal were cultured together. As for negative and positive controls, 2×10^5 labeled lymphocytes were cultured in medium or medium containing concanavalin A (ConA; Sigma). Cells were kept in an incubator at 37°C, 5% CO_2 for 7 days.

At day 7, lymphocytes were collected and stained with anti-bovine CD4 MAb (CACT138A; VMRD). The proliferation of CD4$^+$ T cells was analyzed by measuring the density of PKH67 fluorescence on the live CD4$^+$ T cells via flow cytometry. Data were collected and processed using CellQuest and Modfit LT software (Verity Software House).

Intracellular cytokine staining. PKH67-labeled peripheral blood lymphocytes that had been cocultured with PPD-treated CD11c$^+$ cells for 7 days were harvested and stained for intracellular-cytokine production. Lymphocytes were fixed with 2% paraformaldehyde for 20 min and permeabilized with PermaWash buffer (phosphate-buffered saline containing 0.1% saponin and 0.1% sodium azide) for 10 min. For IFN-γ staining, permeabilized lymphocytes were incubated with mouse anti-bovine IFN-γ MAb (7B6, IgG1; AbD Serotec), followed by PE-conjugated anti-IgG secondary antibody (Invitrogen). For intracellular-IL-4 staining, PE-conjugated mouse anti-bovine IL-4 MAb (CC303, IgG2a; AbD Serotec) was used for the direct labeling. Proper isotype controls were included in the assay. Labeled lymphocytes were then fixed again with 2% paraformaldehyde and analyzed via flow cytometry.

ELISA. Supernatants of lymphocyte and granuloma CD11c$^+$ cell coculture were collected and analyzed for the secretion of IFN-γ by enzyme-linked immunosorbent assay (ELISA). A BOVIGAM (bovine IFN-γ test) kit (CSL Veterinary) was used for the detection of IFN-γ protein in supernatant. Recombinant IFN-γ protein (AbD Serotec) was used as a positive control to generate the standard curve.

Statistical analysis. Data are presented as the mean value ± standard error of the mean except where stated otherwise. The software used for statistical analysis and scientific graph generation included JMP 7 (SAS Institute, Inc.) and GraphPad Prism 4.0 (GraphPad Software, Inc.). Student's *t* test and analysis of variance were used for the statistical analysis. Differences were considered significant if the *P* value was <0.05.

RESULTS

Morphology and cellular composition of *M. avium* subsp. *paratuberculosis*- and vaccine-induced granulomas. Palpable, firm nodules formed at both vaccine and *M. avium* subsp. *paratuberculosis* injection sites by 7 days postinoculation and were removed surgically for analysis. We first set out to determine if early *M. avium* subsp. *paratuberculosis* granulomas had type I or II characteristics in subcutaneous infectious sites. Histologies of granulomatous lesions induced by *M. avium* subsp. *paratuberculosis* or vaccine are shown in Fig. 1A. Mor-

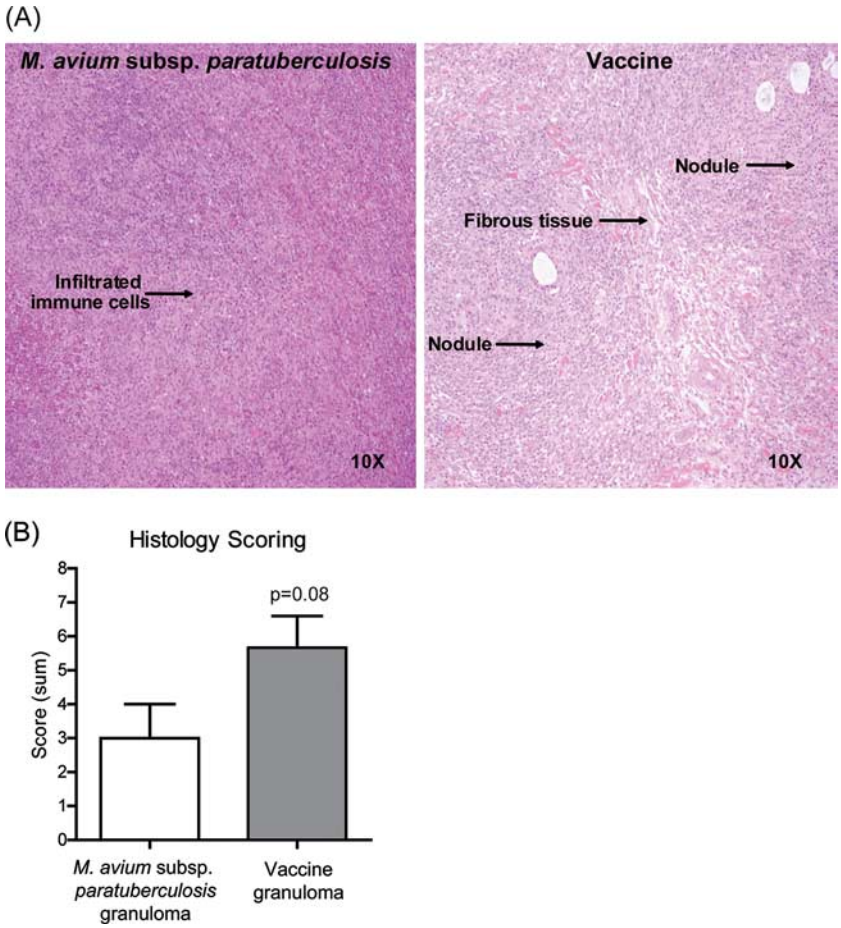

FIG. 1. Histology of granulomatous lesions induced by *M. avium* subsp. *paratuberculosis* or vaccine at 7 days postinoculation. (A) H&E-stained sections of formalin-fixed and paraffin-embedded tissues. Images representative of results from two *M. avium* subsp. *paratuberculosis*-inoculated animals and four vaccinated animals are shown. Original magnification is shown. (B) Lesions were scored from 0 to 3 based on the following individual parameters: mature fibrous connective tissue delineation, macrophage infiltration, lymphocyte organization, multinucleated giant cells, necrosis, and mineralization. Individual parameters were summated, and a single collective score was assigned for each lesion which reflects the histological organization of individual lesions. Pooled data from two *M. avium* subsp. *paratuberculosis*-inoculated animals and four vaccinated animals are shown.

phologically, the *M. avium* subsp. *paratuberculosis* inoculation site consisted of a nearly diffuse infiltration of macrophages intermixed with widely scattered lymphocytes. In contrast, granulomas from vaccine sites had a higher degree of organization, including nodular arrangement of macrophages, discrete collections of perivascular lymphocytes, and fibrous tissue delineation around macrophage aggregates. Lesions were scored based on individual parameters, including fibrous tissue delineation, macrophage infiltrates, and lymphocyte organization. Individual parameters for each lesion were added for a cumulative score, with higher scores corresponding to higher organization. Low-scoring granulomas correlate with type II granulomas, while high-scoring granulomas correlate with type I granulomas. At 7 days postinoculation, there was a trend for *M. avium* subsp. *paratuberculosis* granulomas to have a lower score than the vaccination site granulomas (Fig. 1B). The organization of vaccine, but not *M. avium* subsp. *paratuberculosis*, granulomas increased with time (data not shown). In addition, the individual-parameter scores were significantly lower in *M. avium* subsp. *paratuberculosis* granulomas, including scores for fibrous tissue delineation and lymphocyte organization (data not shown).

We next set out to determine the cellular composition of *M. avium* subsp. *paratuberculosis*- and vaccine-induced granulomas. To accomplish this, total granuloma cells were isolated from granuloma digests and the phenotypes were determined via flow cytometry based on surface marker expression. There were significantly fewer $CD11c^+$ $CD205^+$ cells (DC), $CD14^+$ $CD68^+$ cells (macrophages), and $CD4^+$ T lymphocytes in the *M. avium* subsp. *paratuberculosis*-induced granulomas than in the vaccine granulomas ($P < 0.05$, Fig. 2A). The presence and the number of $CD11c^+$ cells, macrophages, and $CD4^+$ T cells were further confirmed by immunohistochemistry staining (Fig. 2B). The staining frequencies for these cells correlated with the percentages determined by flow cytometry.

Cytokine gene expression in *M. avium* subsp. *paratuberculosis* and vaccine granuloma cells. To better understand the cytokine microenvironment within granulomas, we used LCM to recover total granuloma cells from granuloma cryosections. In these cells, we used qRT-PCR to evaluate the levels of gene

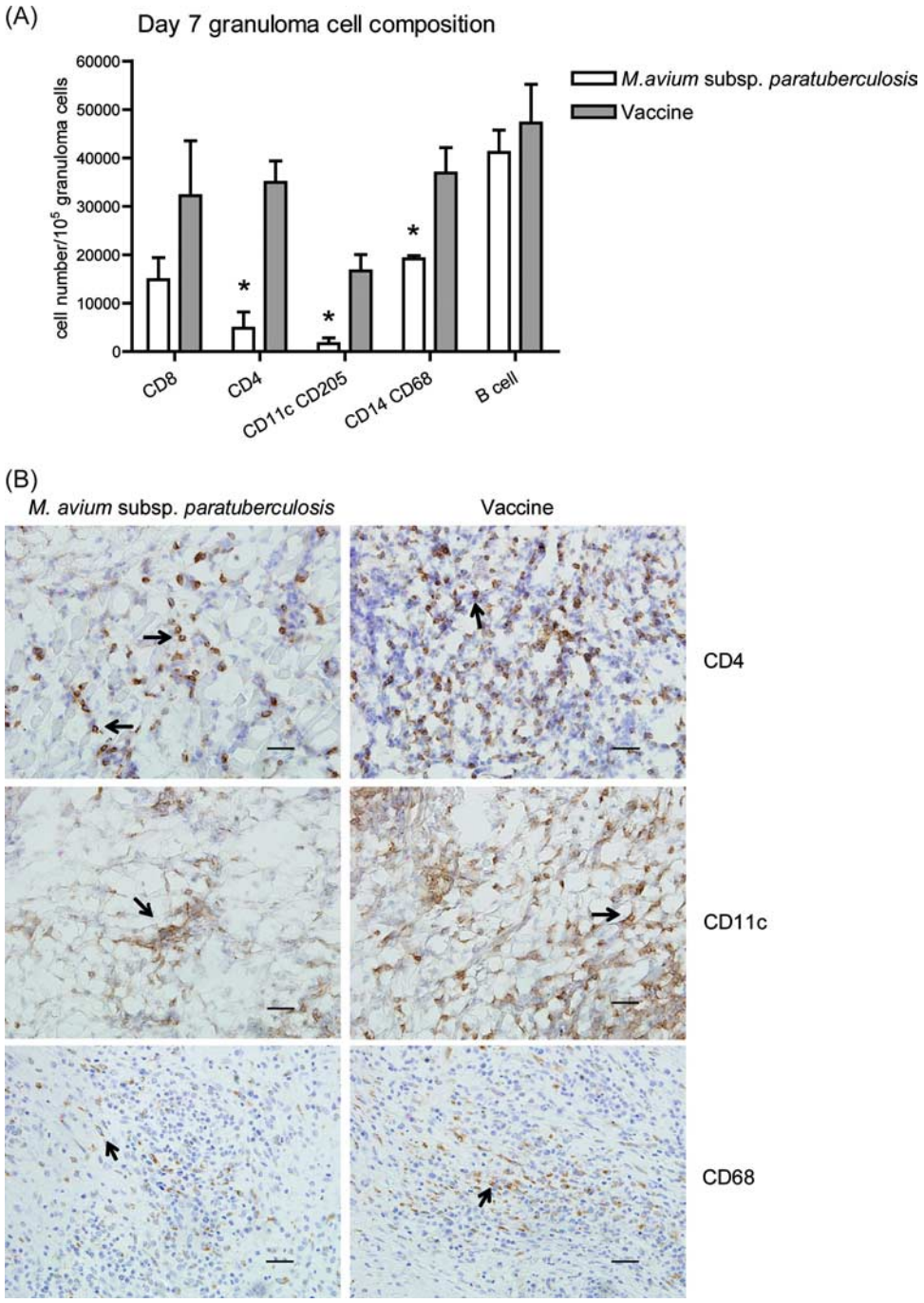

FIG. 2. Cellular composition of granulomas at 7 days postinoculation. (A) Total cells were recovered from granuloma digests. Phenotype was determined by using immunofluorescent staining for surface markers and flow cytometry. Data are the means ± standard errors of the means of the number of cells expressing a surface marker from two *M. avium* subsp. *paratuberculosis*-inoculated animals and four vaccinated animals. *, $P < 0.05$. (B) Granulomatous lesions were immunohistochemically stained for CD4, CD11c (from frozen sections), and CD68 (from formalin-fixed sections). Arrows indicate positive staining for the specific markers. Images representative of results from two *M. avium* subsp. *paratuberculosis*-inoculated animals and four vaccinated animals are shown. Bars represent 50 μm.

expression of a panel of target cytokines that are important for granuloma formation. Cells recovered from *M. avium* subsp. *paratuberculosis*-induced granulomatous lesions expressed significantly lower levels of IFN-γ, TNF-α, and transforming growth factor β (TGF-β) than the cells from vaccine-induced granulomas ($P < 0.05$; Table 2). Both *M. avium* subsp. *paratuberculosis* and vaccine granuloma cells had low levels of IL-4 expression. All data were normalized to the data for internal control β-actin, which was expressed at similar levels within both sets of tissues.

Phenotypic features of granuloma CD11c$^+$ DC. In order to explore the role of antigen-presenting cells within the granu-

TABLE 2. Total granuloma cell cytokine gene expression[a]

Cytokine	Expression (mRNA arbitrary units) in granuloma from:	
	M. avium subsp. *paratuberculosis* inoculation site	Vaccine inoculation site
IFN-γ	41,654.6 ± 21,487	115,129 ± 8,912.8[b]
TNF-α	14.4 ± 10	575 ± 199.1[b]
TGF-β	3.1 ± 3.0	257 ± 65.2[b]
IL-4	0.54 ± 0.48	3.5 ± 3.4

[a] Cytokine gene expression in total granuloma cells from *M. avium* subsp. *paratuberculosis* or vaccine inoculation sites at 7 days postinoculation. Total granuloma cells were isolated from H&E-stained cryosections using LCM, and cytokine gene expression was determined by qRT-PCR. β-Actin was used as an internal control for the assay and was expressed at similar levels in both tissues. Target gene mRNA expression was normalized to β-actin mRNA within the same tissue. Means ± standard errors of the means of results in arbitrary units are shown. Data were generated from two *M. avium* subsp. *paratuberculosis*-inoculated animals and four vaccinated animals.

[b] *P* values of <0.05 were considered to be statistically significant.

loma, we recovered CD11c$^+$ cells from granuloma digests using an AutoMACS column. Isolated CD11c$^+$ cells were evaluated for surface markers associated with an expected DC phenotype. As shown in Fig. 3, granuloma CD11c$^+$ cells expressed low levels of CD14 and medium to high levels of MHC-I and MHC-II molecules, which were independent of the inoculation status. These cells were also positive for CD205 expression (data not shown). This pattern of surface marker expression is consistent with the phenotype reported for bovine DC (23, 25) and DC phenotypes in other species (4, 13, 25, 36).

To analyze the maturation of granuloma DC, LCM was used to capture immunofluorescently labeled CD11c$^+$ cells from granuloma cryosections and the levels of gene expression of costimulatory molecules (CD40, CD80, and CD86) and chemokine receptor (CCR7) were determined via qRT-PCR. *M. avium* subsp. *paratuberculosis* granuloma DC had significantly lower levels of CD40, CD80, CD86, and CCR7 gene expression than the vaccine granuloma DC. This suggests limited DC maturation within the *M. avium* subsp. *paratuberculosis* granuloma relative to DC maturation within the vaccine granuloma (Fig. 4A).

Function of granuloma CD11c$^+$ DC. To assess the function of DC within the granulomas, the cytokine production and ability to induce CD4$^+$ T-cell proliferation of granuloma DC were evaluated. We measured cytokine gene expression in LCM-recovered CD11c$^+$ DC. DC from *M. avium* subsp. *paratuberculosis* granulomas expressed significantly lower levels of IL-10 and IL-12p40 subunit than vaccine granuloma DC (Fig. 4B). To explore antigen presentation, we measured the antigen-specific proliferation of autologous peripheral blood T cells cultured with DC. The DC were recovered from granuloma digests by using an AutoMacs column. Similar numbers of CD4$^+$ T cells were recovered from peripheral blood from vaccinated and *M. avium* subsp. *paratuberculosis*-inoculated animals, which responded similarly to ConA (data not shown and Fig. 5B). Initially, equal numbers of lymphocytes were added to granuloma CD11c$^+$ DC cultures; thus, we started with approximately the same number of CD4$^+$ T cells for each

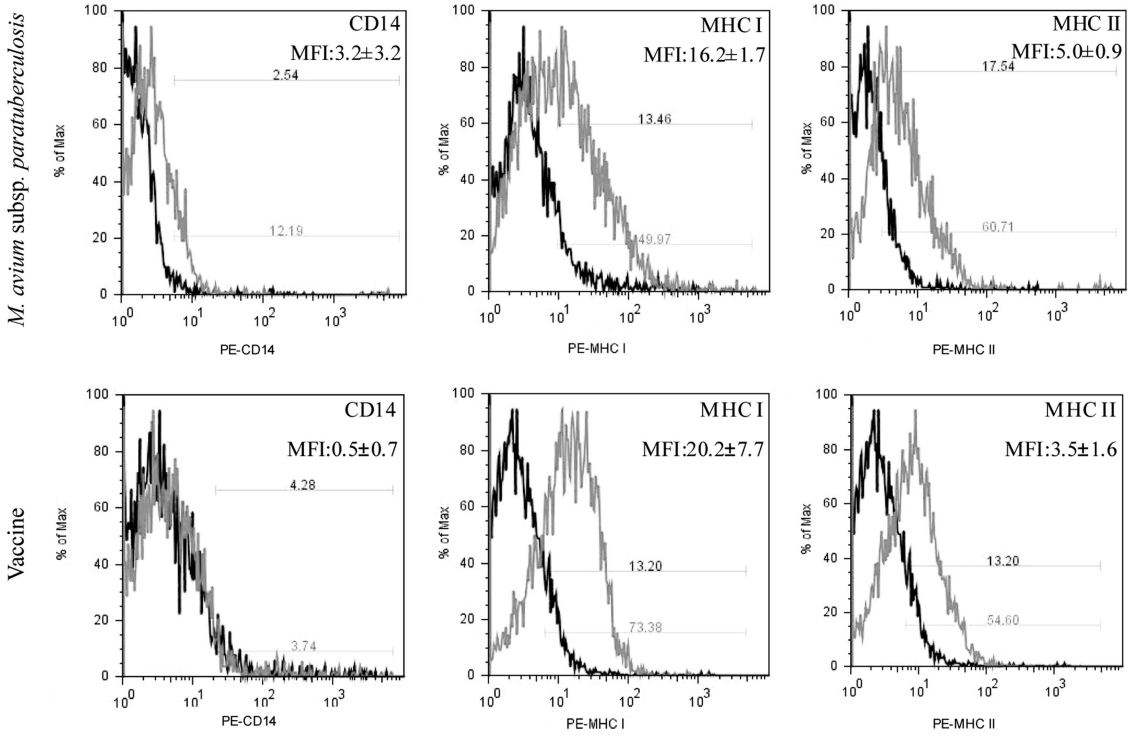

FIG. 3. Surface marker expression on CD11c$^+$ cells recovered from *M. avium* subsp. *paratuberculosis*-induced or vaccine-induced granulomas. CD11c$^+$ cells were isolated from granuloma digests by using an AutoMACS column. CD11c$^+$ cells were then immunofluorescently labeled for CD14, MHC-I, and MHC-II, and labeling was measured by flow cytometry. Surface marker expression is shown in gray, and isotype antibody control is in black. Mean fluorescent intensity (MFI) is listed for each surface marker. Flow cytometry histograms are representative of results for two *M. avium* subsp. *paratuberculosis*-inoculated animals and four vaccinated animals.

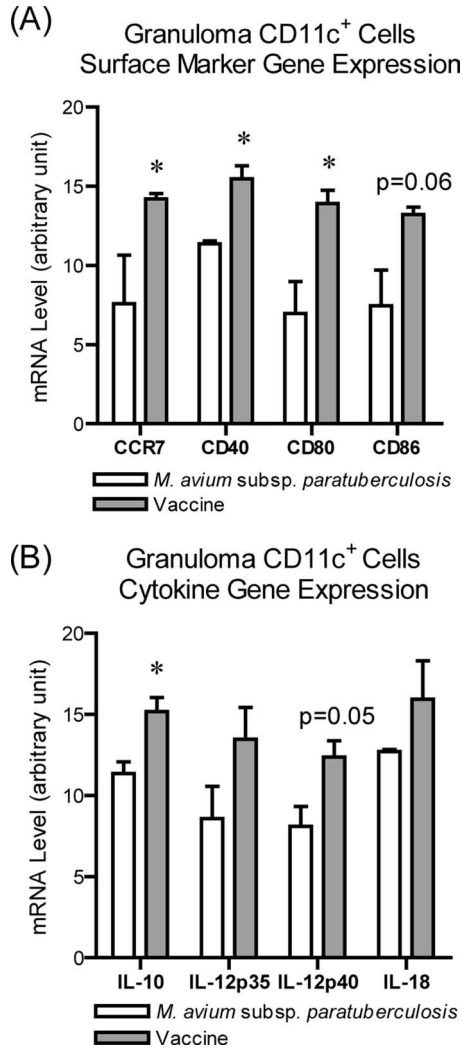

FIG. 4. Granuloma DC expression of costimulatory molecules, chemokine receptors, and cytokines. Granuloma cryosections were labeled for CD11c, and fluorescently labeled cells were captured by using LCM. Gene expression was determined by using qRT-PCR. (A) Levels of gene expression of costimulatory molecules CD40, CD80, and CD86 and the chemokine receptor CCR7 in DC. (B) Gene expression of the cytokines IL-10 and IL-12p40 subunit. β-Actin was the internal control and was expressed at similar levels in both tissues. Target gene mRNA expression was normalized to β-actin mRNA within the same tissue. Statistically significant *P* values as shown are indicated with an asterisk. Data are from two *M. avium* subsp. *paratuberculosis*-inoculated animals and four vaccinated animals.

treatment. After 7 days, 47.7% of lymphocytes cultured with vaccine granuloma DC were $CD4^+$ $PKH67^{dim}$, indicating a proliferated $CD4^+$ T-cell population (Fig. 5A). In contrast, at 7 days 26.5% of the lymphocytes cultured with *M. avium* subsp. *paratuberculosis* granuloma DC were in the proliferated population. The combined data from all animals are shown in Fig. 5B.

To evaluate the ability of DC to polarize proliferating T cells, IL-4 and IFN-γ production by lymphocytes cocultured with granuloma DC was determined by intracellular staining and flow cytometry. In addition, IFN-γ was measured in culture supernatants by using a commercially available ELISA. Approximately 18% of total lymphocytes were in the $PKH67^{dim}$ IL-4^+ population after culture with the vaccine granuloma DC (Fig. 6A). In contrast, *M. avium* subsp. *paratuberculosis* granuloma DC did not induce significant IL-4 production. The proportions of IFN-γ-producing lymphocytes in the proliferative population ($PKH67^{dim}$) were similar in both vaccine and *M. avium* subsp. *paratuberculosis* granuloma DC treatments (Fig. 6B). Supernatants from vaccine DC-lymphocyte cocultures contained significantly higher levels of IFN-γ than those from *M. avium* subsp. *paratuberculosis* granuloma DC-lymphocyte cocultures ($P < 0.05$). There is a disparity between the lymphocyte intracellular staining and ELISA results with respect to IFN-γ. In these cultures, we would identify some degree of IFN-γ from nonproliferated cells ($PKH67^{bright}$), as well as production of IFN-γ by CD4-negative cells. These contributions would account for the levels of IFN-γ in the culture supernatants being higher than those in the intracellular staining and indicate that, overall, vaccine granuloma DC induced the highest levels of IFN-γ production and secretion.

DISCUSSION

A fundamental step in the pathogenesis of disease caused by *M. avium* subsp. *paratuberculosis* is the formation of lepromatous or type II granulomas within the intestine during the late stages of infection. This provides an environment for nearly unrestricted pathogen proliferation and facilitates shedding of *M. avium* subsp. *paratuberculosis* into the environment. Although our understanding of the immunopathology of late disease is more complete, we have a very limited understanding of the early events within the intestine after exposure to *M. avium* subsp. *paratuberculosis*. In cattle, it has been difficult to identify *M. avium* subsp. *paratuberculosis* or intestinal granulomas within the first few months after experimental oral infection. It has been reported that the initial immune response following exposure to mycobacterial pathogens, including DC-pathogen interactions, is critical in generating sustained protective immunity (9). DC have recently been shown to be critical to granuloma formation within the intestine, and therefore, DC are likely have a key role in the generation of local protection to *M. avium* subsp. *paratuberculosis* during the initial period after infection (28). By understanding the early events in granuloma development after subcutaneous exposure to *M. avium* subsp. *paratuberculosis*, we believe we gain some insight into the local immune response during this early period within the intestine. In this study, we compared subcutaneous granulomas that developed in response to *M. avium* subsp. *paratuberculosis* to those that developed in response to an inducer of type I granulomas, focusing on granuloma formation in relation to DC function. To induce type I granulomas, we used a commercially available *M. avium* subsp. *paratuberculosis* vaccine that induces strong cell-mediated immune responses both at the inoculation site and systemically. It has a field efficacy that is reported to be as high as 90% (54). It is likely that the success of this vaccine is, in part, due to the strong local immune response it induces at the inoculation site.

In this study, the early *M. avium* subsp. *paratuberculosis* granulomas lacked features of a type I granuloma, including nodular arrangement of macrophages, fibrous delineation, and

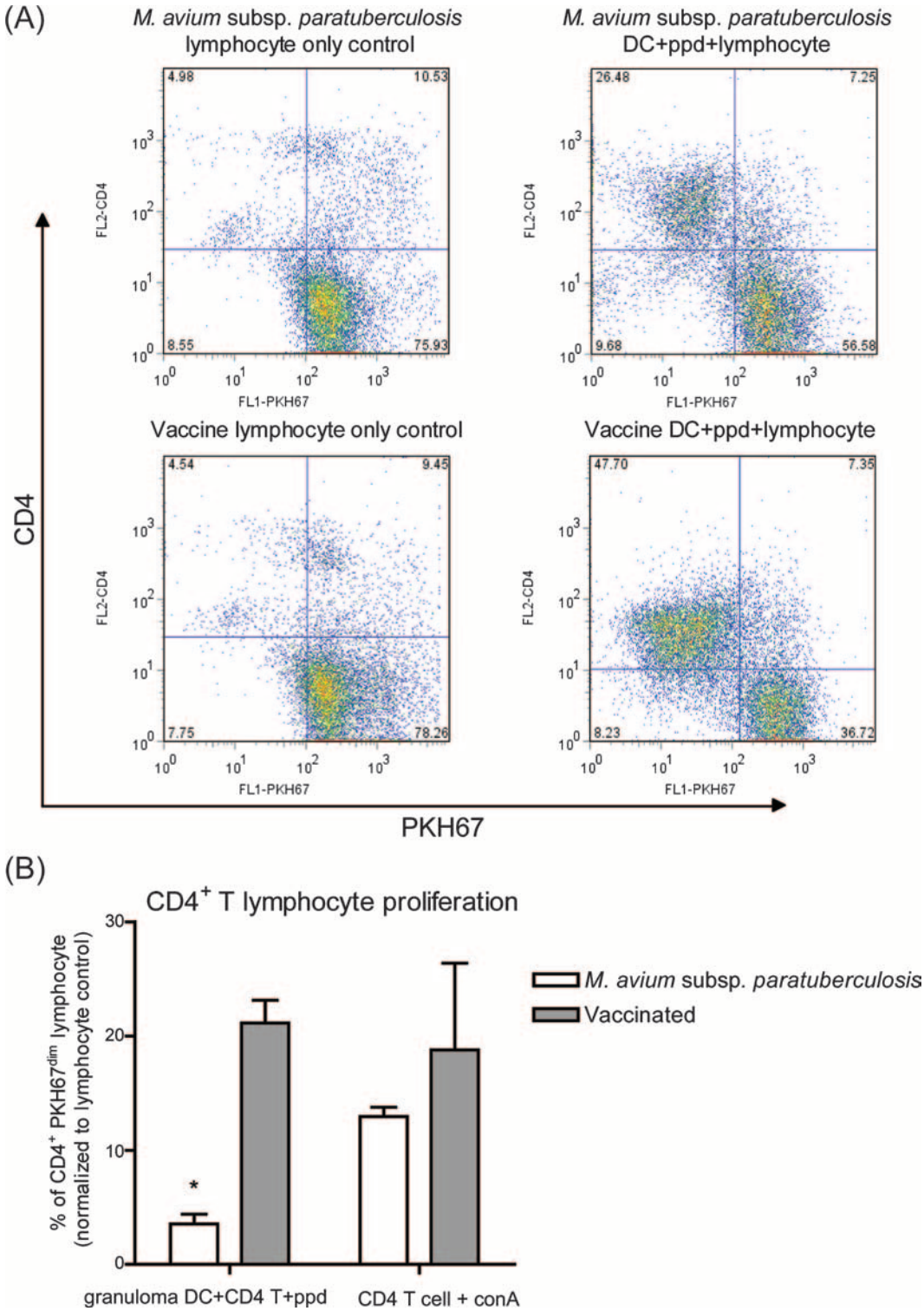

FIG. 5. Granuloma DC-induced proliferation of autologous peripheral blood lymphocytes. (A) DC were isolated from *M. avium* subsp. *paratuberculosis* or vaccine granuloma digests by using an AutoMACS column, based on CD11c expression, and pulsed with PPD overnight. Autologous lymphocytes were labeled with PKH67 and cultured for 7 days with DC. (B) The percentage of PKH67^{dim} (proliferated-cell populations) was divided by the percentage of PKH67^{dim} cells in the negative controls (lymphocytes cultured alone). Combined data from two *M. avium* subsp. *paratuberculosis*-inoculated and four vaccinated animals are shown. Numbers in the quadrants represent percentages of cells relative to the total number of cells. FL1, PKH67 fluorescence; FL2, PE-CD4 fluorescence; *, $P < 0.05$.

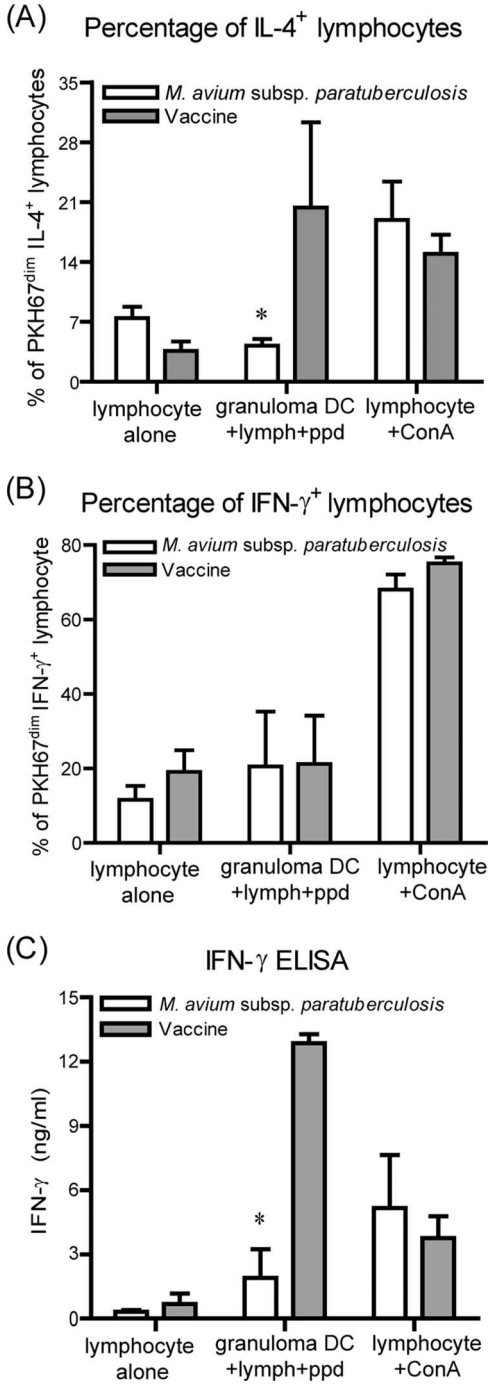

FIG. 6. Lymphocyte cytokine production after coculture with granuloma DC. (A) PKH67-labeled lymphocytes were cocultured for 7 days with granuloma DC. After 7 days, the cells were labeled for intracellular IL-4. Graph depicts numbers of lymphocytes that are $PKH67^{dim}$ and IL-4 positive. (B) PKH67-labeled lymphocytes were cocultured for 7 days with granuloma DC. After 7 days, the cells were labeled for intracellular IFN-γ. Graph depicts numbers of lymphocytes that were $PKH67^{dim}$ and IFN-γ positive. (C) Levels of IFN-γ in the supernatants of lymphocyte-DC cocultures were determined by ELISA. Data are from results for two *M. avium* subsp. *paratuberculosis*-inoculated animals and four vaccinated animals. *, $P < 0.05$.

organization of lymphoid infiltrates at an early time point, 7 days postinfection. In contrast, the vaccine site had these type I features, which became progressively more prominent with time. It is plausible, based on these findings, that the granulomatous response that initially develops in the intestine at the *M. avium* subsp. *paratuberculosis* infection site also lacks morphological features of protective type I granulomas. $CD4^+$ T cells have been shown to be important in the development of granulomas during mycobacterial infection, including the development of the strong local Th1 immune responses required for granuloma function (16, 27, 32, 37). The levels of $CD4^+$ T cells were significantly lower in the *M. avium* subsp. *paratuberculosis* granulomas than in the vaccine granulomas. DC are more-recently recognized as an important cellular constituent of the granuloma. We are beginning to understand that DC within the granuloma participate in granuloma development and function through their ability to recruit inflammatory cells, present antigen to infiltrating T cells, and migrate to draining nodes (34, 53). Long-term latency has been shown to be associated with DC interaction with organized lymphoid tissue within and adjacent to pulmonary *M. tuberculosis* granulomas (53). Reduced numbers of DC within the *M. avium* subsp. *paratuberculosis* granulomas suggest potential limitations in these activities that optimally would drive type I granuloma formation.

TNF-α and IFN-γ are essential cytokines in developing and sustaining granuloma morphology and function (42, 44). In the current study, low levels of IFN-γ are likely related to fewer $CD4^+$ T cells within the *M. avium* subsp. *paratuberculosis* granuloma. $CD4^+$ T cells are major contributors to IFN-γ production at sites of mycobacterial infection, which is one mechanism by which they support pathogen control locally (16). It has been shown that TNF-α-deficient mice infected with *M. tuberculosis* cannot clear the infection and die due to widespread bacterial dissemination. Importantly, the granulomas in $TNF^{-/-}$ mice infected with *M. tuberculosis* were poorly organized (3, 26). Considering the effects of TNF-α on the cytokine and chemokine cascades and cellular infiltration and organization, a low level of TNF-α gene expression early in *M. avium* subsp. *paratuberculosis* infection may contribute to a lack of granuloma organization. The relatively high levels of expression of TGF-β, IL-4, and IL-10 in the vaccine granulomas are consistent with a local host response to limit excessive inflammation. These cytokines coincided with a high level of IFN-γ within the granuloma, which has been shown to play an important regulating role in granulomas through negative-feedback mechanisms (8).

To better understand the influence of DC on granuloma formation, we explored the phenotypes of $CD11c^+$ DC isolated from vaccine and *M. avium* subsp. *paratuberculosis* granulomas. DC costimulatory molecule and chemokine receptor expression levels were significantly lower in the DC recovered from *M. avium* subsp. *paratuberculosis* granulomas. However, MHC-I and MHC-II expression levels were similar for DC from both granuloma types. One explanation for this observation is that the DC from the *M. avium* subsp. *paratuberculosis* granuloma had undergone some degree of maturation, but not the full maturation of the vaccine granuloma DC. Incomplete maturation of DC has been reported for DC infected with mycobacteria, as well as bystander DC in vitro (10, 29, 31). We

have recently reported that bovine monocyte-derived DC are permissive to infection with *M. avium* subsp. *paratuberculosis* in vitro, which interferes with complete DC maturation (25). It is plausible that *M. avium* subsp. *paratuberculosis* infection of bovine DC in vivo also interferes with complete DC maturation. Incomplete DC maturation in vivo would result in a reduced ability to present antigen both within the granuloma and in draining lymph nodes, thereby favoring pathogen persistence. Additionally, the DC isolated from *M. avium* subsp. *paratuberculosis* and vaccine granulomas likely consisted of both antigen-encountered maturing DC and newly recruited immature DC. Thus, the DC phenotype may also reflect the degree of DC turnover within the infection site. DC in vaccine granulomas had higher levels of CCR7 gene expression. CCR7 is important for DC migration to secondary lymphoid tissues (41). This suggests that the ability of vaccine DC to traffic to lymphoid tissues is stronger than that of DC from *M. avium* subsp. *paratuberculosis* granulomas.

Vaccine granuloma DC had the strongest ability to induce T-cell proliferation. This corresponds to higher levels of gene expression of costimulatory molecules and proinflammatory cytokines and suggests that the antigen presentation capability is stronger than that of the DC from the *M. avium* subsp. *paratuberculosis* granulomas. We used autologous peripheral blood lymphocytes as the T-cell source, and proliferation was likely due to both naïve and memory T-cell stimulation. We consider the T-cell proliferation at 7 days postinfection to consist largely of naïve T cells, with a smaller contribution from memory T cells. Equal numbers of $CD4^+$ T cells were recovered from vaccine- and *M. avium* subsp. *paratuberculosis*-challenged animals, each with similar and strong proliferative responses to ConA. This suggests that *M. avium* subsp. *paratuberculosis* infection did not overtly interfere with systemic $CD4^+$ T-cell responses in these animals and that DC function was the major contributor to differences in T-cell proliferation. These data point to DC from within the *M. avium* subsp. *paratuberculosis* granuloma as having a diminished ability, in comparison to that of vaccine granuloma DC, to successfully present antigen. The enhanced T-cell proliferation induced by vaccine granuloma DC was associated with higher levels of gene expression of IL-12p40 by these DC. IL-12 is important in driving T-cell polarization and proliferation by DC (56). Another factor that may account for the lower number of $CD4^+$ T cells after their culture with DC from the *M. avium* subsp. *paratuberculosis* animals is increased T-cell death. The signal between CD28 on T cells and CD80 and CD86 on DC has been shown to be critical in preventing T-cell death (7, 33). Thus, it is possible that $CD4^+$-T-cell death may relate to the lower levels of costimulatory-molecule expression on the *M. avium* subsp. *paratuberculosis* granuloma DC.

In summary, subcutaneous *M. avium* subsp. *paratuberculosis* or vaccine administration resulted in the formation of distinct granulomas with unique cellular and cytokine profiles. Importantly, vaccine granulomas had higher numbers of $CD4^+$ T cells and DC with increased expression of both TNF-α and IFN-γ. These differences corresponded to significant differences in the phenotypes and functional responses of DC from within the granuloma. Specifically, the DC from the *M. avium* subsp. *paratuberculosis* granulomas had lower levels of expression of costimulatory and chemokine receptors, suggesting limited maturation. This DC phenotype was associated with lower T-cell proliferation. Taken together, these findings suggest that *M. avium* subsp. *paratuberculosis* infection in vivo influences DC function, which may further shape the developing granuloma. We acknowledge that differences in the components of the inoculum (adjuvants, etc.) influence the local immune response and, consequently, we do not assign all granuloma attributes to DC function. However, we believe this work demonstrates important DC characteristics that coincide with the induction of protective immune responses to *M. avium* subsp. *paratuberculosis.* This may provide insight into how sustained protection against *M. avium* subsp. *paratuberculosis* fails at the local innate level during natural disease.

ACKNOWLEDGMENTS

We thank Weiwei Zhang and Elise Huffman for their technical assistance.

This work was funded through grants from the Iowa Livestock Health Advisory Council, USDA Animal Plant Health Inspection Service, and the Healthy Livestock Initiative of Iowa.

REFERENCES

1. **Adams, L. B., and J. L. Krahenbuhl.** 1996. Granulomas induced by Mycobacterium leprae. Methods **9:**220–232.
2. **Algood, H. M., J. Chan, and J. L. Flynn.** 2003. Chemokines and tuberculosis. Cytokine Growth Factor Rev. **14:**467–477.
3. **Bean, A. G., D. R. Roach, H. Briscoe, M. P. France, H. Korner, J. D. Sedgwick, and W. J. Britton.** 1999. Structural deficiencies in granuloma formation in TNF gene-targeted mice underlie the heightened susceptibility to aerosol Mycobacterium tuberculosis infection, which is not compensated for by lymphotoxin. J. Immunol. **162:**3504–3511.
4. **Bodnar, K. A., N. V. Serbina, and J. L. Flynn.** 2001. Fate of *Mycobacterium tuberculosis* within murine dendritic cells. Infect. Immun. **69:**800–809.
5. **Chiodini, R. J., and C. D. Buergelt.** 1993. Susceptibility of Balb/c, C57/B6 and C57/B10 mice to infection with Mycobacterium paratuberculosis. J. Comp. Pathol. **109:**309–319.
6. **Chiu, B. C., C. M. Freeman, V. R. Stolberg, J. S. Hu, E. Komuniecki, and S. W. Chensue.** 2004. The innate pulmonary granuloma: characterization and demonstration of dendritic cell recruitment and function. Am. J. Pathol. **164:**1021–1030.
7. **Collette, Y., A. Benziane, D. Razanajaona, and D. Olive.** 1998. Distinct regulation of T-cell death by CD28 depending on both its aggregation and T-cell receptor triggering: a role for Fas-FasL. Blood **92:**1350–1363.
8. **Cooper, A. M., D. K. Dalton, T. A. Stewart, J. P. Griffin, D. G. Russell, and I. M. Orme.** 1993. Disseminated tuberculosis in interferon gamma gene-disrupted mice. J. Exp. Med. **178:**2243–2247.
9. **Dieli, F., N. Caccamo, S. Meraviglia, J. Ivanyi, G. Sireci, C. T. Bonanno, V. Ferlazzo, C. La Mendola, and A. Salerno.** 2004. Reciprocal stimulation of gammadelta T cells and dendritic cells during the anti-mycobacterial immune response. Eur. J. Immunol. **34:**3227–3235.
10. **Dulphy, N., J. L. Herrmann, J. Nigou, D. Rea, N. Boissel, G. Puzo, D. Charron, P. H. Lagrange, and A. Toubert.** 2007. Intermediate maturation of Mycobacterium tuberculosis LAM-activated human dendritic cells. Cell. Microbiol. **9:**1412–1425.
11. **Ehlers, S.** 2005. Why does tumor necrosis factor targeted therapy reactivate tuberculosis? J. Rheumatol. Suppl. **74:**35–39.
12. **Emile, J. F., N. Patey, F. Altare, S. Lamhamedi, E. Jouanguy, F. Boman, J. Quillard, M. Lecomte-Houcke, O. Verola, J. F. Mousnier, F. Dijoud, S. Blanche, A. Fischer, N. Brousse, and J. L. Casanova.** 1997. Correlation of granuloma structure with clinical outcome defines two types of idiopathic disseminated BCG infection. J. Pathol. **181:**25–30.
13. **Fach, S. J., S. L. Brockmeier, L. A. Hobbs, H. D. Lehmkuhl, and R. E. Sacco.** 2006. Pulmonary dendritic cells isolated from neonatal and adult ovine lung tissue. Vet. Immunol. Immunopathol. **112:**171–182.
14. **Flynn, J. L., and J. Chan.** 2005. What's good for the host is good for the bug. Trends Microbiol. **13:**98–102.
15. **Flynn, J. L., M. M. Goldstein, J. Chan, K. J. Triebold, K. Pfeffer, C. J. Lowenstein, R. Schreiber, T. W. Mak, and B. R. Bloom.** 1995. Tumor necrosis factor-alpha is required in the protective immune response against Mycobacterium tuberculosis in mice. Immunity **2:**561–572.
16. **Guidry, T. V., R. L. Hunter, Jr., and J. K. Actor.** 2007. Mycobacterial glycolipid trehalose 6,6′-dimycolate-induced hypersensitive granulomas: contribution of CD4+ lymphocytes. Microbiology **153:**3360–3369.
17. **Hostetter, J., E. Huffman, K. Byl, and E. Steadham.** 2005. Inducible nitric oxide synthase immunoreactivity in the granulomatous intestinal lesions of naturally occurring bovine Johne's disease. Vet. Pathol. **42:**241–249.

18. **Hueber, A. J., and I. B. McInnes.** 2007. Immune regulation in psoriasis and psoriatic arthritis: recent developments. Immunol. Lett. **114:**59–65.
19. **Iyonaga, K., K. M. McCarthy, and E. E. Schneeberger.** 2002. Dendritic cells and the regulation of a granulomatous immune response in the lung. Am. J. Respir. Cell Mol. Biol. **26:**671–679.
20. **Jayapal, V., K. M. Sharmila, G. Selvibai, S. P. Thyagarajan, N. Shanmugasundaram, and S. Subramanian.** 1991. Fluorescein diacetate and ethidium bromide staining to determine the viability of Mycobacterium smegmatis and Escherichia coli. Lepr. Rev. **62:**310–314.
21. **Johnson, L., J. Gough, Y. Spencer, G. Hewinson, M. Vordermeier, and A. Wangoo.** 2006. Immunohistochemical markers augment evaluation of vaccine efficacy and disease severity in bacillus Calmette-Guerin (BCG) vaccinated cattle challenged with Mycobacterium bovis. Vet. Immunol. Immunopathol. **111:**219–229.
22. **Lammas, D. A., E. De Heer, J. D. Edgar, V. Novelli, A. Ben-Smith, R. Baretto, P. Drysdale, J. Binch, C. MacLennan, D. S. Kumararatne, S. Panchalingam, T. H. Ottenhoff, J. L. Casanova, and J. F. Emile.** 2002. Heterogeneity in the granulomatous response to mycobacterial infection in patients with defined genetic mutations in the interleukin 12-dependent interferon-gamma production pathway. Int. J. Exp. Pathol. **83:**1–20.
23. **Langelaar, M. F., J. C. Hope, V. P. Rutten, J. P. Noordhuizen, W. van Eden, and A. P. Koets.** 2005. Mycobacterium avium ssp. paratuberculosis recombinant heat shock protein 70 interaction with different bovine antigen-presenting cells. Scand. J. Immunol. **61:**242–250.
24. **Larsen, A. B., A. I. Moyle, and E. M. Himes.** 1978. Experimental vaccination of cattle against paratuberculosis (Johne's disease) with killed bacterial vaccines: a controlled field study. Am. J. Vet. Res. **39:**65–69.
25. **Lei, L., and J. Hostetter.** 2007. Limited phenotypic and functional maturation of bovine monocyte-derived dendritic cells following Mycobacterium avium subspecies paratuberculosis infection in vitro. Vet. Immunol. Immunopathol. **120:**177–186.
26. **Lin, P. L., H. L. Plessner, N. N. Voitenok, and J. L. Flynn.** 2007. Tumor necrosis factor and tuberculosis. J. Investig. Dermatol. Symp. Proc. **12:**22–25.
27. **Little, D., H. M. Alzuherri, and C. J. Clarke.** 1996. Phenotypic characterisation of intestinal lymphocytes in ovine paratuberculosis by immunohistochemistry. Vet. Immunol. Immunopathol. **55:**175–187.
28. **Mizoguchi, A., A. Ogawa, H. Takedatsu, K. Sugimoto, Y. Shimomura, K. Shirane, K. Nagahama, T. Nagaishi, E. Mizoguchi, R. S. Blumberg, and A. K. Bhan.** 2007. Dependence of intestinal granuloma formation on unique myeloid DC-like cells. J. Clin. Investig. **117:**605–615.
29. **Motta, A., C. Schmitz, L. Rodrigues, F. Ribeiro, C. Teixeira, T. Detanico, C. Bonan, H. Zwickey, and C. Bonorino.** 2007. Mycobacterium tuberculosis heat-shock protein 70 impairs maturation of dendritic cells from bone marrow precursors, induces interleukin-10 production and inhibits T-cell proliferation in vitro. Immunology **121:**462–472.
30. **Muller, P. Y., H. Janovjak, A. R. Miserez, and Z. Dobbie.** 2002. Processing of gene expression data generated by quantitative real-time RT-PCR. BioTechniques **32:**1372–1379.
31. **Murray, R. A., M. R. Siddiqui, M. Mendillo, J. Krahenbuhl, and G. Kaplan.** 2007. Mycobacterium leprae inhibits dendritic cell activation and maturation. J. Immunol. **178:**338–344.
32. **Navarro, J. A., G. Ramis, J. Seva, F. J. Pallares, and J. Sanchez.** 1998. Changes in lymphocyte subsets in the intestine and mesenteric lymph nodes in caprine paratuberculosis. J. Comp. Pathol. **118:**109–121.
33. **Noel, P. J., L. H. Boise, J. M. Green, and C. B. Thompson.** 1996. CD28 costimulation prevents cell death during primary T cell activation. J. Immunol. **157:**636–642.
34. **Ohteki, T., H. Tada, K. Ishida, T. Sato, C. Maki, T. Yamada, J. Hamuro, and S. Koyasu.** 2006. Essential roles of DC-derived IL-15 as a mediator of inflammatory responses in vivo. J. Exp. Med. **203:**2329–2338.
35. **Ordway, D., M. Henao-Tamayo, I. M. Orme, and M. Gonzalez-Juarrero.** 2005. Foamy macrophages within lung granulomas of mice infected with Mycobacterium tuberculosis express molecules characteristic of dendritic cells and antiapoptotic markers of the TNF receptor-associated factor family. J. Immunol. **175:**3873–3881.
36. **Paillot, R., F. Laval, J. C. Audonnet, C. Andreoni, and V. Juillard.** 2001. Functional and phenotypic characterization of distinct porcine dendritic cells derived from peripheral blood monocytes. Immunology **102:**396–404.
37. **Palmer, M. V., W. R. Waters, and T. C. Thacker.** 2007. Lesion development and immunohistochemical changes in granulomas from cattle experimentally infected with Mycobacterium bovis. Vet. Pathol. **44:**863–874.
38. **Pfaffl, M. W.** 2001. A new mathematical model for relative quantification in real-time RT-PCR. Nucleic Acids Res. **29:**e45.
39. **Plessner, H. L., P. L. Lin, T. Kohno, J. S. Louie, D. Kirschner, J. Chan, and J. L. Flynn.** 2007. Neutralization of tumor necrosis factor (TNF) by antibody but not TNF receptor fusion molecule exacerbates chronic murine tuberculosis. J. Infect. Dis. **195:**1643–1650.
40. **Qiu, B., K. A. Frait, F. Reich, E. Komuniecki, and S. W. Chensue.** 2001. Chemokine expression dynamics in mycobacterial (type-1) and schistosomal (type-2) antigen-elicited pulmonary granuloma formation. Am. J. Pathol. **158:**1503–1515.
41. **Riol-Blanco, L., N. Sanchez-Sanchez, A. Torres, A. Tejedor, S. Narumiya, A. L. Corbi, P. Sanchez-Mateos, and J. L. Rodriguez-Fernandez.** 2005. The chemokine receptor CCR7 activates in dendritic cells two signaling modules that independently regulate chemotaxis and migratory speed. J. Immunol. **174:**4070–4080.
42. **Roach, D. R., A. G. Bean, C. Demangel, M. P. France, H. Briscoe, and W. J. Britton.** 2002. TNF regulates chemokine induction essential for cell recruitment, granuloma formation, and clearance of mycobacterial infection. J. Immunol. **168:**4620–4627.
43. **Russell, D. G.** 2007. Who puts the tubercle in tuberculosis? Nat. Rev. Microbiol. **5:**39–47.
44. **Salgame, P.** 2005. Host innate and Th1 responses and the bacterial factors that control Mycobacterium tuberculosis infection. Curr. Opin. Immunol. **17:**374–380.
45. **Saunders, B. M., and W. J. Britton.** 2007. Life and death in the granuloma: immunopathology of tuberculosis. Immunol. Cell Biol. **85:**103–111.
46. **Serbina, N. V., T. P. Salazar-Mather, C. A. Biron, W. A. Kuziel, and E. G. Pamer.** 2003. TNF/iNOS-producing dendritic cells mediate innate immune defense against bacterial infection. Immunity **19:**59–70.
47. **Simutis, F. J., N. F. Cheville, and D. E. Jones.** 2005. Investigation of antigen-specific T-cell responses and subcutaneous granuloma development during experimental sensitization of calves with Mycobacterium avium subsp paratuberculosis. Am. J. Vet. Res. **66:**474–482.
48. **Simutis, F. J., D. E. Jones, and J. M. Hostetter.** 2007. Failure of antigen-stimulated gammadelta T cells and CD4+ T cells from sensitized cattle to upregulate nitric oxide and mycobactericidal activity of autologous Mycobacterium avium subsp. paratuberculosis-infected macrophages. Vet. Immunol. Immunopathol. **116:**1–12.
49. **Tam, M. A., and M. J. Wick.** 2004. Dendritic cells and immunity to Listeria: TipDC are a new recruit. Trends Immunol. **25:**335–339.
50. **Tanaka, S., M. Sato, T. Onitsuka, H. Kamata, and Y. Yokomizo.** 2005. Inflammatory cytokine gene expression in different types of granulomatous lesions during asymptomatic stages of bovine paratuberculosis. Vet. Pathol. **42:**579–588.
51. **Tsuchiya, T., K. Chida, T. Suda, E. E. Schneeberger, and H. Nakamura.** 2002. Dendritic cell involvement in pulmonary granuloma formation elicited by bacillus calmette-guerin in rats. Am. J. Respir. Crit. Care Med. **165:**1640–1646.
52. **Ulrichs, T., and S. H. Kaufmann.** 2006. New insights into the function of granulomas in human tuberculosis. J. Pathol. **208:**261–269.
53. **Ulrichs, T., G. A. Kosmiadi, S. Jorg, L. Pradl, M. Titukhina, V. Mishenko, N. Gushina, and S. H. Kaufmann.** 2005. Differential organization of the local immune response in patients with active cavitary tuberculosis or with nonprogressive tuberculoma. J. Infect. Dis. **192:**89–97.
54. **Uzonna, J. E., P. Chilton, R. H. Whitlock, P. L. Habecker, P. Scott, and R. W. Sweeney.** 2003. Efficacy of commercial and field-strain Mycobacterium paratuberculosis vaccinations with recombinant IL-12 in a bovine experimental infection model. Vaccine **21:**3101–3109.
55. **Wangoo, A., L. Johnson, J. Gough, R. Ackbar, S. Inglut, D. Hicks, Y. Spencer, G. Hewinson, and M. Vordermeier.** 2005. Advanced granulomatous lesions in Mycobacterium bovis-infected cattle are associated with increased expression of type I procollagen, gammadelta (WC1+) T cells and CD 68+ cells. J. Comp. Pathol. **133:**223–234.
56. **Watford, W. T., M. Moriguchi, A. Morinobu, and J. J. O'Shea.** 2003. The biology of IL-12: coordinating innate and adaptive immune responses. Cytokine Growth Factor Rev. **14:**361–368.